Selective Adsorption of Fe (III) Using Calcium Alginate-Polyacrylamide/Titanium Dioxide Nanocomposites Prepared by Gamma Irradiation

Mai M. Mohamed[1], 1El-Sayed A. Hegazy, H. Kamal[1], El-Sayed A. Soliman[2]

ABSTRACT

Calcium alginate-polyacrylamide/titanium dioxide (CA-PAM/TiO$_2$) nanocomposite biofilms were prepared by solution casting followed by gamma irradiation as initiator. N,N' Methylene bis acrylamide (MBAM) and CaCl$_2$ were used as covalent and ionic crosslinker, respectively. Characterization of the prepared films was performed by XRD and SEM. Adsorption of Fe (III) ions was carried out by batch experiment under varying operating conditions such as, TiO$_2$ content, pH, time, initial metal concentration, temperature and number of adsorption cycles in order to optimize the adsorption conditions for selective removal of Fe (III) from aqueous medium. Atomic absorption spectrophotometer was used to determine the adsorption behavior. Thermodynamic studies of Fe (III) adsorption were also evaluated and indicated that adsorption is chemical and endothermic in nature. Selective adsorption of Fe (III) was studied in the presence of Co (II) and Cu (II) ions as interfering ions. It was found that the selectivity coefficient of the CA-PAM/TiO$_2$ for Fe(III) was 55 and 220 toward Cu (II) and Co (II), respectively. Such values are much higher than that of CA-PAM of composition 50/50 wt% without TiO$_2$ nanoparticle which was 13.3 and 40 also toward Cu (II) and Co (II), respectively. It is concluded that such prepared materials are of interest for practical uses in the removal of Fe (III) from waste water.

1. Polymer Chemistry Department, National Centre for Radiation Research and Technology, Atomic Energy Authority AEA. P.O. Box 29, Nasr City, Cairo, Egypt

2. Chemistry Department, Faculty of Science, Ain shams University, Cairo, Egypt.

INTRODUCTION

Iron is an essential element for all living systems as it is required for respiratory pigments, proteins and many enzymes but the gradual accumulation of Iron leads to a number of diseases as excess of iron in body causes liver and kidney damage. Iron is important in several industrial activities such as the production of pure iron oxide which has a wide range of application in electronic industry **(Teke *et al*., 2004)**. Fe (III) in natural waters present in low levels with interfering metal ions **(Xie *et al*., 2012)**. Therefore, it is of great importance to develop a new sorbent for selective separation of trace amount Fe (III) from natural waters. Adsorption seems to be best methods to decrees heavy metal pollution because of its efficiency, flexibility, simplicity, and low waste production **(Poursani *et al*., 2016).**

Polymer nanocomposites are considered as a suitable material for adsorption of heavy metal from water **(Yin and Deng, 2015) (Lofrano *et al*., 2016).** One of the most interesting methods to prepare polymer nanocomposites is through irradiation of aqueous solution of polymer in presence of well dispersed nanoparticles. Among the most commonly used energy sources for irradiation of polymers is gamma radiation which emitted from ^{60} Co or ^{137} Cs and characterized by its short wavelengths and high-intensity **(Foox *et al*., 2016)**. Gamma-irradiation has been successfully used to prepare polymer nanocomposites in one-step synthesis **(Gasaymeh *et al*., 2010)** and facilitate interaction between polymer components **(Hegazy *et al*., 2015).**

Metal oxides are often used to extend or improve polymer functional properties **(El Sayed *et al*., 2015).** Titanium dioxide (TiO_2) is a naturally occurring oxide of the element titanium also referred to as titania **(Peters *et al*., 2014)**. Titanium dioxide (TiO_2) is an inert, nontoxic and cheap material **(Oleyaei *et al*., 2016)** and can be used for a variety of applications including self-cleaning, water treatment, antibacterial, and air purification**.** It was found that composites containing TiO_2 have a good capability to adsorb heavy metals from aqueous solutions **(Poursani *et al*., 2016)**.

Alginates are a broad family of biodegradable natural polymer that produced from brown seaweeds and soil bacteria **(Rhim and Wang, 2013; Cerqueira *et al*., 2012)**. It exhibits poor water resistance due to hydrophilicity owing to presence of carboxylic and hydroxyl groups. To overcome this, alginate has been crosslinked with polyvalent metal cations like Ca^{2+} **(Benavides *et al*., 2012).** The abundant functional groups in the alginate polymer enhance the adsorption of metal ions.

PAM hydrogel is biocompatible and has soft and wet macroporous structure. The abundant amide functional groups in PAM can form strong interactions with Sodium alginate to form blend film with desired properties **(El Miri *et al*., 2015)** which can easily performed by gamma radiation **(Dey *et al*., 2014)**.

This work aims to prepare calcium alginate-polyacrylamide (CA-PAM) blend film with excellent mechanical performances by mixing covalently crosslinked acrylamide (AM) and ionically crosslinked sodium alginate (SA) using gamma irradiation and incorporation of different TiO_2 nanoparticle contents (wt%) to determine the selective adsorption of Fe (III) from aqueous solutions.

EXPERIMENTAL

Materials

Sodium alginate purchased from Qualikems Laboratory Reagent made in India, **Acrylamide** obtained from (Merck, Germany), Methylene bis acrylamide AR was purchased from Oxford Laboratory Reagent, India, Calcium chloride anhydrous was purchased from Qualikems Laboratory Reagent India, and **Glycerol** $C_3H_8O_3$ was purchased from Piochem for Laboratory Chemicals. Titanium

dioxide TiO_2; (**nano**-powder) was produced from Sigma-Aldrich Co. with average particle size of 21 nm. All chemicals were used as received without further purification. Different salts of heavy metal ions were used in the metal uptake measurements such as $CuCl_2$, $FeCl_3$, and $CoCl_2$ and were purchased from Qualikems Laboratory Reagent, India.

Gamma radiation source

Irradiation of samples was carried out using a ^{60}Co gamma source Egypt, with average dose rate of 2.70127 kGy/h and total dose 10 kGy.

Preparation of CA-PAM/TiO$_2$ Nanocomposite Films

Different concentrations of TiO_2 nanoparticles (0.1-0.5 wt%) were dispersed in 25 ml of water and stirred for 1 h, and then sonicated in an ultrasonic bath (Ps-series model) for 3 h. It was not possible to prepare nanocomposites with TiO_2 content higher than >0.5 wt% in order to prevent the nanoparticles agglomeration. Nanocomposite films form solutions were prepared by slowly adding TiO_2 to the dissolved solution of SA-AAM (50/50 wt%) during stirring process, 40 % glycerol and 3% MBAM as crosslinker were added. The film solutions were then casted onto 5 plastic Petri dishes and irradiated at 10 kGy by ^{60}Co gamma radiation as more than this dose, severe degradation of Calcium alginate as natural polymer occur. So we selected 10 kGy as a moderate dose for this investigation. After irradiation films left to dry in oven at 40°C for 24h and then immersed in 1% $CaCl_2$ for 2h to introduce ionic species.

Crystallinity Measurements

XRD measurements were carried out at room temperature to investigate the change in crystallinity of polymer. X-ray diffraction pattern (intensity vs. diffraction angle plate) was recorded in the range of diffraction angle $2\theta = 10\text{-}80^O$ at a scan speed of 8°/min using (XRD-6000) with Cu-target.

Surface Topography Measurements

The surface of the nanocomposite films were examined using scanning electron microscopy (SEM), JEOL JSM-5400, Japan. The surface of the samples was sputter-coated with gold before examination.

pH Measurement

The pH of the solutions that used for the treatment experiments was measured using advanced pH meter **(ORION EA 940).** Adjusting different pH 1-3 by using stock solution HCl (1%)

Batch Adsorption Studies of Fe (III)

The adsorption of Fe (III) onto CA-PAM/TiO$_2$ nanocomposite films was investigated by batch experiments through immersing certain weight of nanocomposites in 25 mL of $FeCl_3$ solution. Effect of TiO_2 content, pH, initial Fe (III) concentration, and temperature on adsorption behavior was studied.

The amount of Iron remaining after adsorption time was determined using Unicam- 939 atomic absorption spectrophotometer (England).

The amount of metal adsorbed was calculated using the following equation **(Golkhah et al., 2017)**

$$q_e = \frac{(c_o - c_e)V}{W}$$

where q_e is the amount adsorbed per unit mass of the adsorbent (mg/g); C_o and C_e are the initial and equilibrium concentration of Fe (III) (ppm), respectively; V is the volume of $FeCl_3$ solution (L); W is the weight of the adsorbent (g).

Reusability and Regeneration Efficiency %

Certain weight of metal ions loaded films were immersed in 20 mL 1%HCl solution for 2 h at room temperature. Then the metal ions free film was reused in another removal process of Fe (III) in initial concentration 30 ppm. The process was repeated in four times and amount of adsorbed metal ion calcu-

lated every time of adsorption and the regeneration efficiency (RE) was determined using the following equation **(Thakur, 2017)**

$$RE = \frac{\text{Metal adsorbed in } 2^{nd} \text{ time}}{\text{Metal adsorbed in } 1^{st} \text{ time}} \; X \; 100$$

Adsorption Selectivity test for Fe (III) in case of Competitive Adsorption with Interfering Co (II) and Cu (II) Metal Ions

The study of adsorption selectivity was carried out by adding certain amount of adsorbent into 25 mL of mixture solution containing Fe (III), Co(II), and Cu (II) at initial concentration of 90 ppm and the concentration of each metal ion of 30 ppm for each ion. This study was carried out for both CA-PAM and CA-PAM/TiO$_2$ nanocomposite film.

Distribution coefficient (K$_d$), selectivity coefficient (k) of the adsorbent used were calculated by the following equations 6, 7 **(Xie *et al*., 2012).**

$$K_d = \frac{q_e}{C_e}$$

$$K = \frac{K_d \; Fe(III)}{K_d \; Cu(II) \; or \; Co \; (II)}$$

RESULTS AND DISCUSSION

The synthesized film with different content of TiO$_2$ nanoparticles was noted as CA-PAM/TiO$_2$ nanocomposite film and the film without adding TiO$_2$ was noted as CA-PAM. Introduction of TiO$_2$ to CA-PAM films may cause certain changes in crystallinity and surface morphology of CA-PAM films as shown from characterization studies.

Characterization

XRD of pure TiO$_2$ and CA-PAM/TiO$_2$ Nanocomposites

XRD pattern of pure TiO$_2$ and CA-PAM/TiO$_2$ nanocomposite films contain different TiO$_2$ concentrations are shown in Fig.1.
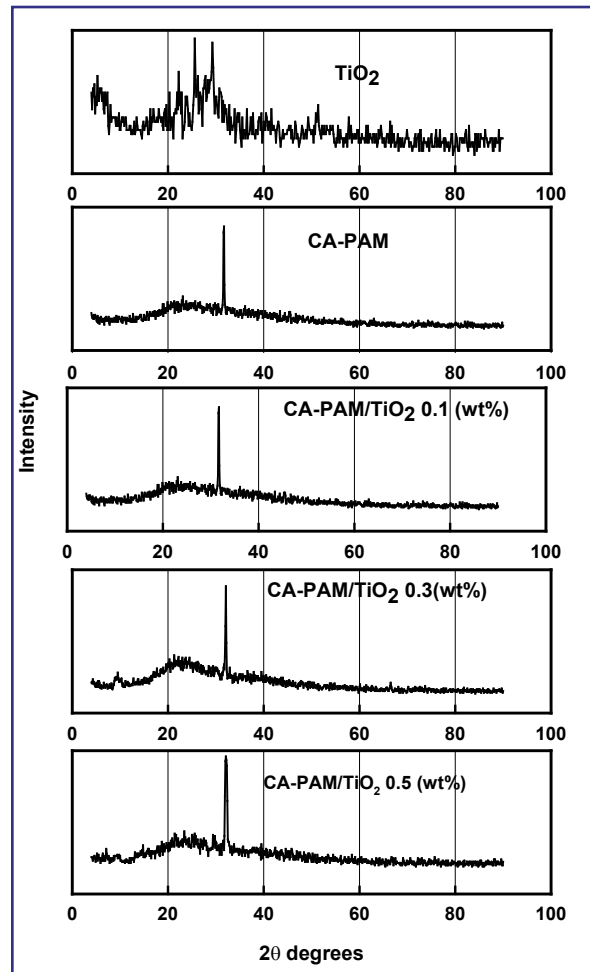

Fig. (1): XRD patterns of CA-PAM and CA-PAM/TiO$_2$ nanocomposite films with different contents of TiO$_2$ nanoparticles.

XRD pattern of TiO$_2$ exhibited a characteristic broad and weak intense peaks appeared at 2θ values of 25.5, 29.2, and 26.1, 22.5, 8.22, 9.7, 16.2, 51.1 which indicate amorphous structure of TiO$_2$. Most peaks of TiO$_2$ are disappeared with nanocomposite indicating the dispersion of TiO$_2$ nanoparticles inside the film matrix and strong interaction occurs between TiO$_2$ and polymer network **(Borai *et al*., 2015)**.

The weak intense peak at around 2θ=29◦ in the XRD pattern of TiO$_2$ nanoparticles was appeared in XRD pattern of CA-PAM/TiO$_2$ nanocomposites but were shifted to higher 2θ value of 31.8, 31.84, and 30 at TiO$_2$ content of 0.1, 0.3 and 0.5 wt%, respectively. This may confirm the incorporation and fine

dispersion of TiO_2 in the film matrix. The shift in 2θ at highest concentration of nanoparticles to lower value compared to the low concentration of nanoparticles can be attributed to the agglomeration of excess TiO_2 which make a decrease in the crystallinity of nanoparticles inside nanocomposite film matrix **(Norranattrakul et al., 2013)**. Also with increasing TiO_2 content to 0.3 wt% a new diffraction peak was appeared at $2\theta= 9\circ$ which attributed to the presence of TiO_2 in the film matrix. With increasing TiO_2 concentration up to 0.5 wt%, peak intensity at 2θ $9\circ$ is slightly reduced indicating an extensive interaction between different components of the film with TiO_2 nanoparticles, and if there was no compatibility in the nanocomposite films, each component had its own crystal region in the film **(Oleyaei et al., 2016)**.

The presence of TiO_2 0.1% in the CA-PAM film causes some process of disorder and shifts the diffraction peak at $2\theta = 31.72$ towards lower values (31.62º) which indicate the decrease of crystallinity compared to CA-PAM film without TiO_2 due to

polymer suffer from structural rearrangement **(Eisa et al., 2011)** at first addition of TiO_2 nanoparticles but at TiO_2 content 0.3 and 0.5 wt% the diffraction peak shifts the towards higher values of 2θ to become 31.8, and 32.1º, respectively which indicate increase of crystallinity and formation of more ordered structure **(El Sayed et al., 2015)**

In order to evaluate size of nanoparticles, the apparent crystalline dimensions along the 101 lattice direction were calculated by measuring the width at half –height of the corresponding Bragg reflection and applying Sherr model **(Paranhos et al., 2007)**:

$L_\theta=K\lambda/\beta Cos\ \theta$

Where L_θ is the apparent crystalline dimension along a given lattice direction, k is the Scherr constant (k=0.89 rad), λ is the wavelength of the X-rays (0.154 nm), β is the width at half-height (expressed in radians), and θ is the Bragg angle. The results are shown in Table 1.

Table (2) : *Crystalline parameters of pure TiO_2 and the prepared CA-PAM/TiO_2 film with different concentrations of TiO_2 nanoparticles.*

Sample	2θ (degree)	d-spacing(nm)	L_θ (nm)
Pure TiO$_2$	29.22	3.05	34.65
CA/PAM/TiO$_2$ (0.1%)	31.80	2.81	90.8
CA/PAM/TiO$_2$ (0.3%)	31.84	2.80	27.7
CA/PAM/TiO$_2$ (0.5%)	30	2.97	74.9

By considering the characteristic peak for TiO_2 in the diffraction pattern at $2\theta= 29º$, the mean crystal sizes of TiO_2 in the CA-PAM film containing 0.1, 0.3 and 0.5% TiO_2 were 93.8 and 27.7 nm, 74.9, respectively. The average crystallite size of TiO_2 nanoparticles is 34.6 nm, and the reason for size increment of TiO_2 within the nanocomposite films may be attributed to agglomeration of TiO_2 nanoparticles **(Oleyaei et al., 2016)** so decrease in the interlayer basal

spacing of TiO_2 nanoparticles inside the nanocomposite films compared to pure TiO_2 nanoparticles.

Surface Topography of Prepared Nanocomposites

SEM was used to study surface topography of the prepared films. Figure 2 shows SEM images of CA-PAM, and CA-PAM/TiO_2 nanocomposites.

a) CA-PAM

b) CA-PAM/TiO$_2$ 0.1 (wt%)
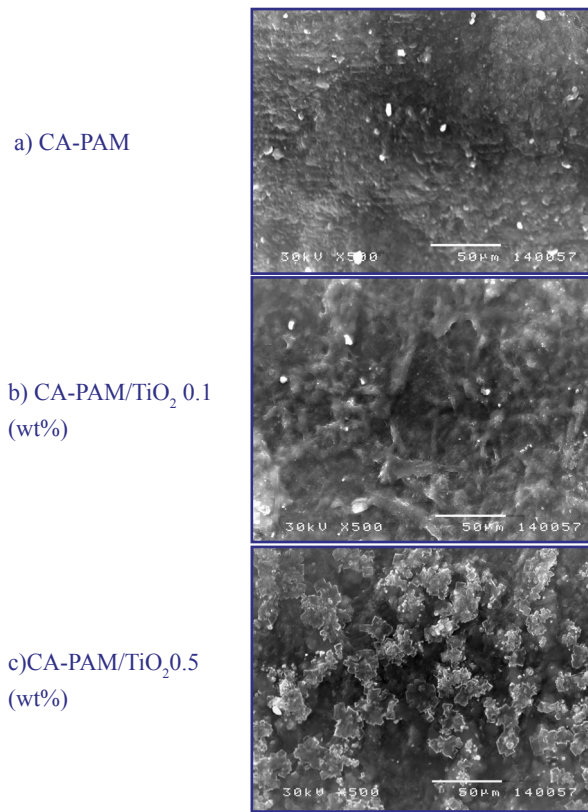
c)CA-PAM/TiO$_2$0.5 (wt%)

Fig. (2): SEM of CA-PAM, CA-PAM/TiO$_2$ nanocomposite films.

It can be seen that the homogeneity and smoothness of the CA-PAM film surface decreased with the addition of TiO$_2$ nanoparticles and many pores were distributed uniformly on the surface of nanocomposite films leading to large surface area and porous structure. However, the presence of high TiO$_2$ concentration (0.5 wt%) results in presence of some aggregation due to formation of agglomerated cluster-like structures due to the presence of high inorganic nanoparticle contents **(Atta *et al*., 2016)**. It may be concluded that the concentration of TiO$_2$ affects nanocomposite film morphology as it transformed from fibrous to particle pattern with increasing TiO$_2$ content **(Basavarajav *et al*., 2010).**

Adsorption studies of Fe (III)

Effect of Time on Removal % of Fe (III)

Removal % of Fe (III) ions was investigated as a function of adsorption time and the results are shown in Fig. 3. It was found that the removal % increased rapidly in the beginning time of adsorption process till 120 min which can be attributed to the abundant amount of vacant active sites on the surface of the adsorbents, which are occupied by the metal ion as time passes **(Karkeh-abadi *et al*., 2016).** Then the removal % becomes almost stable indicating that equilibrium state achieved between the adsorbate solutions and adsorbents. It was concluded that time required to achieve maximum Fe (III) adsorption is 120 min.
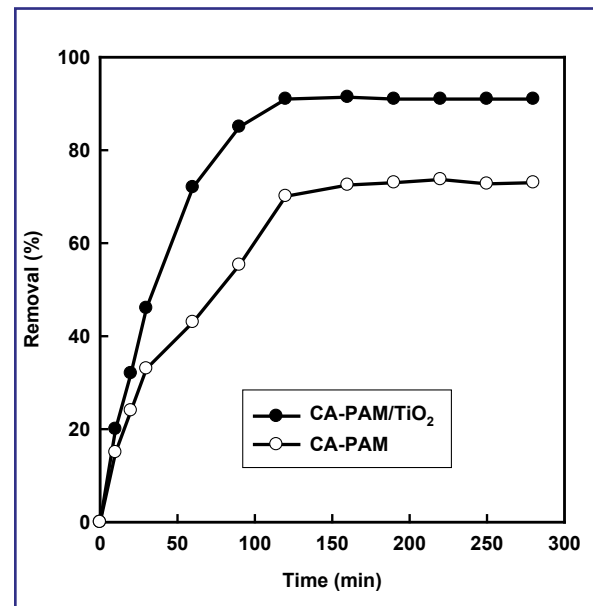

Fig. (3): Time profile of Fe (III) adsorption by CA-PAM and CA-PAM/TiO$_2$ nanocomposite films, TiO$_2$ content; 0.3 (wt%), initial metal concentration; 30 ppm, and pH; 3.

Effect of pH on Adsorption of Fe (III)

Among important parameters affecting adsorption is pH of the aqueous solution as the binding of metal ions by surface functional groups is strongly pH-dependent **(Bouhamed *et al*., 2014).** The existence and contents of ions (H$^+$ either or OH$^-$) in the acidic and basic solutions depend on the pH, which can directly affect the anionic nature of adsorbent and adsorbate molecules **(Karkeh-abadi *et al*., 2016).** The experiments were performed at different pHs 1-3. It was found that with increasing pH greater than 3, poor solubility of the Fe salts is observed

Selective Adsorption of Fe (III) Using Calcium Alginate-Polyacrylamide/Titanium Dioxide
Nanocomposites Prepared by Gamma Irradiation

(57)

(**Mittal *et al.*, 2015**). The removal % of Fe (III) by CA-PAM and CA-PAM/TiO$_2$ nanocomposite films contain 0.3 wt% of TiO$_2$ is investigated at different pH values and the results are shown in Fig. 4.
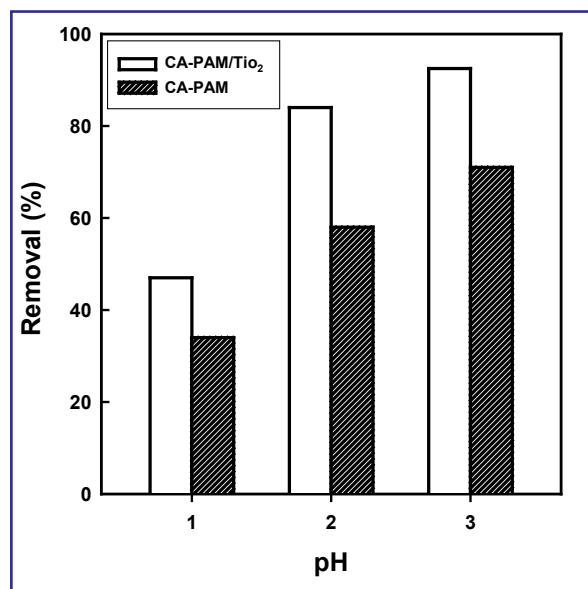

Fig. (4): Effect of pH on Fe (III) removal by CA-PAM and CA-PAM/TiO$_2$ nanocomposite, TiO$_2$ content 0.3 wt%, initial metal concentration; 30 ppm, contact time; 2h, at 25°C.

It is observed that by increasing pH from 1 to 3 resulted in increasing the Fe (III) removal % by both CA-PAM and CA-PAM/TiO$_2$ nanocomposite films. This can be explained on the basis that the solution pH affects the ionization state of polymer functional groups. So at low pH, large quantities of coexisting H$^+$ ions present that can be adsorbed on the polymer functional groups and competed with metal ions for the surface of the adsorbent, so little amount of Fe (III) adsorbed due to the repulsion with H$^+$ (**Mittal *et al.*, 2015**). However, with increasing pH, adsorption increases as the H$^+$ ions content decreases providing a greater chance for Fe (III) to successfully interact with the adsorption active sites and subsequently increases the removal % (**Moniera *et al.*, 2015).** Also increasing the pH resulted in deprotonation of functional groups allowing metal ion to interact with binding sites on polymer surface (**Quintelas *et al.*, 2009)**. At all the pH values, CA-PAM/TiO$_2$ nanocomposite film is more efficient adsorbent than CA-

PAM and exhibited higher removal %.

2.3. Effect of TiO$_2$ Concentration on Removal % of Fe (III)

Adsorption phenomenon includes the reactions between adsorbate and adsorbent (**Pal *et al*, 2015**). Iron (III) is an important metal and it is of great importance to develop a new adsorbent for selective removal of Fe (III) from aqueous solution (**Xie *et al.*, 2012**). At first, adsorption of Fe (III) was studied at different experimental conditions. Figure 5 shows the effect of TiO$_2$ nanoparticles content (wt%) on removal % of Fe (III).
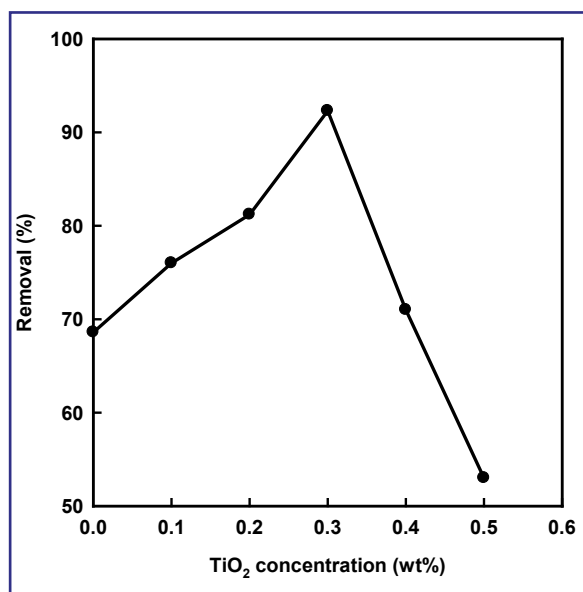

Fig. (5): Effect of TiO$_2$ concentration on removal % of Fe (III) from aqueous solution by CA-PAM/TiO$_2$ nanocomposite films of composition 50/50 (wt%), initial metal concentration; 30 ppm, pH 3, and contact time; 2h at 25°C.

It was concluded that the concentration of TiO$_2$ in nanocomposite films is an important factor affecting Fe (III) adsorption. It was observed that, percent removal of Fe (III) increases with increasing TiO$_2$ content due to its relatively high surface and abundant functional groups which enhance the uptake process (**Borai *et al.*, 2015**). Maximum removal percent is 91.2 % which attained by CA-PAM/TiO$_2$ nanocomposite film containing 0.3 wt% of TiO$_2$ nanoparticles. The decrease of Fe (III) removal % at

nanoparticle concentration higher than 0.3% because nanoparticles can be considered as a crosslinker in the reaction and presence of high concentration of TiO_2 nanoparticles greater than 0.3 wt% resulted in increasing the crosslinking density of the nanocomposite. Therefore, more compact network structure formed thus the spaces left for metal ion adsorption decreased **(Borai *et al.*, 2015)**

Effect of Initial Fe (III) Concentration on Adsorption Capacity

A series of Iron chloride solution with different concentrations (10 - 50 mg/L) were prepared. The variation of adsorption capacity with initial concentration of Fe (III) is shown in Fig. 6.
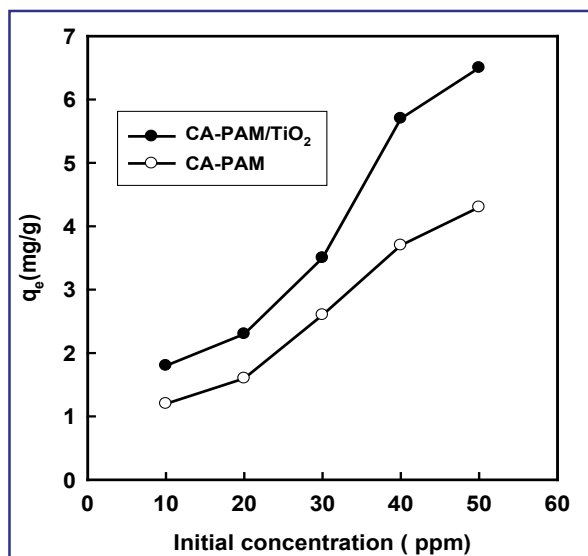

Fig. (6): Effect of initial Fe (III) concentration on adsorption capacity using CA-PAM and CA-PAM/TiO_2 nanocomposite films with TiO_2 content; 0.3 wt%, contact time 120 min, at pH 3.

As initial concentration increases from 10-50 ppm the adsorption capacity increases from 1.2 to 4.3 mg g^{-1} in case of adsorption by CA-PAM and from 1.8-6.5 mg g^{-1} in case of adsorption by CA-PAM/TiO_2 nanocomposite film. Increasing adsorption capacity with increasing Fe (III) may be attributed to the increasing the driving force which allows diffusion of metal ions to inside the film matrix and increasing interaction between adsorbent and adsorbate **(Mittal *et al.*, 2015).** Surface saturation was

dependent on the initial metal ion concentration. At low concentration due to the available adsorption sites which can easily interact with Fe (III), but at higher concentrations, the metal ions have to diffuse into the polymer surface by intraparticle diffusion and this process is slow **(Quintelas *et al.*, 2009)**.

Effect of Temperature and Thermodynamic Studies

Adsorption of Fe (III) by CA-PAM and CA-PAM/TiO_2 nanocomposite films was investigated at temperature range from 30 to 55°C and the results are shown in Fig.7.
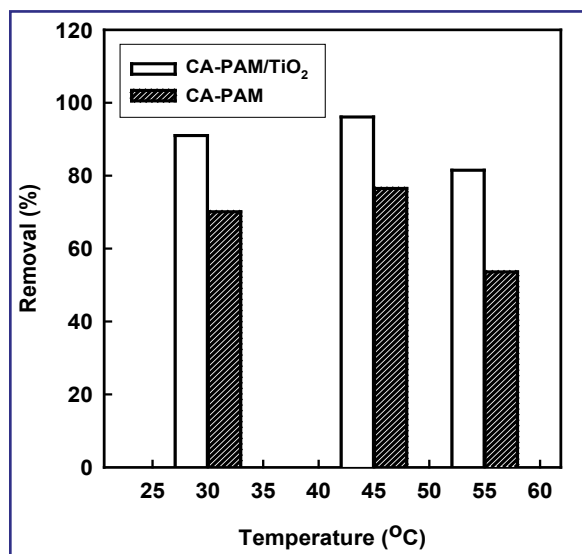

Fig. (7): Effect of temperature on Fe (III) adsorption by CA-PAM and CA-PAM/TiO_2 nanocomposite films, TiO_2 content; 0.3 (wt%), initial metal concentration; 30 ppm, pH; 3 and contact time 2h.

The removal percent of Fe (III) slightly increases with increasing temperature from 20 to 45°C**.** The increase in Fe (III) adsorption may be due to enhance the mobility of metal ions with increasing temperature as well as greater activity of binding sites as temperature increases. At temperatures higher than 45°C, the adsorption of metal ions decreases. This may be attributed to the damaging of adsorbent surface **(Golkhah *et al.*, 2017)**.

Thermodynamic studies give more information about the inherent energetic changes involved during adsorption **(Karkeh-abadi *et al.*, 2016)**. The

Selective Adsorption of Fe (III) Using Calcium Alginate-Polyacrylamide/Titanium Dioxide
Nanocomposites Prepared by Gamma Irradiation

(59)

enthalpy change of adsorption (ΔH) was calculated using the following thermodynamic equation (**Abou Taleb** *et al.*, **2009**):

$$\ln\left(\frac{C_{e2}}{C_{e1}}\right) = \left(\frac{\Delta H}{R}\right)\left[\left(\frac{1}{T_1}\right) - \left(\frac{1}{T_2}\right)\right]$$

Where C_{e1} and C_{e2} are the equilibrium concentrations Fe (III) at absolute temperature T_1 and T_2, respectively where R is the universal gas constant=8.314 J/ (mol. K).

Figure 8 shows ln C_e versus 1/T, in which the slope of these graph give ΔH/R values. The enthalpy change value of adsorption (ΔH) was found to be 204 and 299 KJ/mol for CA-PAM and CA-PAM/TiO₂ nanocomposite films, respectively. The positive value of ΔH indicates that the reaction is endothermic and consumes energy in the adsorption process (**Selçuk** *et al.*, **2017**). The enthalpy change value (ΔH) for physical adsorption is smaller than that of chemical adsorption. Typically, ΔH for physical adsorption ranges from 0-40 KJ/mol and of chemical adsorption ranging from 40-800 KJ/mol (**Abou Taleb** *et al.*, **2009**).The obtained results clarified that the uptake of Fe (III) on the prepared films is chemisorption. It is also obvious that the adsorption en-
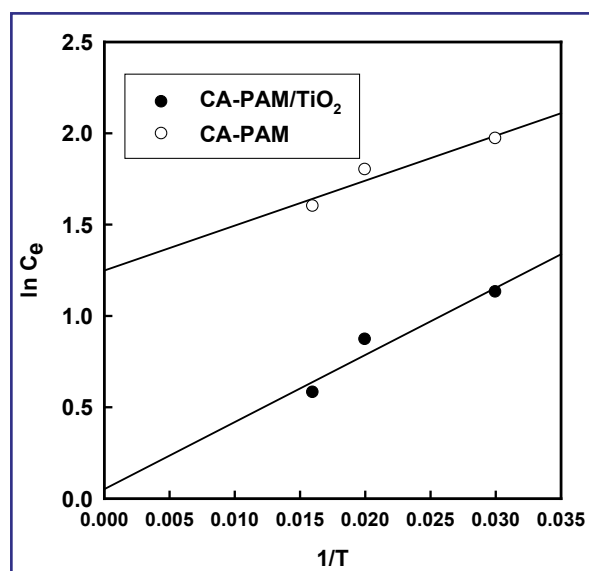
thalpy change for CA-PAM/TiO₂ is larger than that of CA-PAM. It means that the interaction between Fe (III) and nanocomposite film is stronger and then leads to an enhanced adsorption.

Reusability Test

In view of practical application, the adsorbent should be chemically stable after several repeated adsorption treatments (**Habiba** *et al.*, **2016**). An efficient adsorbent should exhibit excellent adsorption capacity in addition to good regeneration characteristics to make the adsorbents economically Valuable (**Pal** *et al.*, **2015**). The repeated use, i.e., regenerability, of the adsorbent is an important factor in improving process economics. For this reason, desorption of the adsorbed metal ions from the films was also studied in a batch experimental set-up. The films loaded with maximum amounts of Fe (III) were regenerated through immersing in desorption medium containing 1.0 M HCl and the corresponding products after desorption were washed with distilled water, dried and reused again for metal adsorption process. The adsorption–desorption process was repeated in four cycles with initial metal concentration 30 ppm. In each cycle the amount of the adsorbed Fe (III) on CA-PAM and CA-PAM/TiO₂ nanocomposite films was measured and the results are represented in Fig. 9.

Fig. (8): Variation of lnC$_e$ of CA-PAM and CA-PAM/TiO₂ nanocomposite films for adsorption of Fe (III) with 1/T.
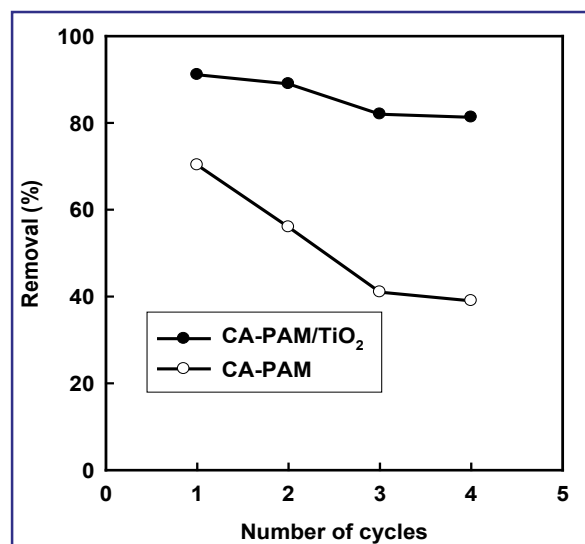

Fig. (9): Cycling runs of Fe (III) adsorption by CA-PAM and CA-PAM/TiO₂ nanocomposite films.

The two main mechanisms which occur simultaneously during the uptake of heavy metal ions are:

(i)   electrostatic interactions or van der Waals force of attraction

(ii)   Covalent bond interaction like ion exchange or chelation.

It was monitored that desorption of metal ions occur by ion exchange between metal and H^+ (of HCL) on the polymer surface **(Pal *et al.*, 2015)**. It was found that CA-PAM/TiO$_2$ nanocomposite film is more stable under the experimental process and exhibits excellent reusability than CA-PAM which is a key factor in practical application. As lack in amount of Fe (III) adsorbed by CA-PAM/TiO$_2$ nanocomposite film after four adsorption process is less than that observed in adsorption by CA-PAM film so nanocomposite film maintains about 90 % of its original efficiency after final cycle and CA-PAM film maintain only 50%

Selectivity Studies of Fe (III) Adsorption

Mixture of known amount of two interfering metal ions Cu (II), and Co (II) allowed competing Fe (III) adsorption by CA-PAM and CA-PAM/TiO$_2$ nanocomposite films. Residual amounts of each metal ion remaining after adsorption were determined using atomic absorption spectroscopy and the results are shown in Fig. 10.
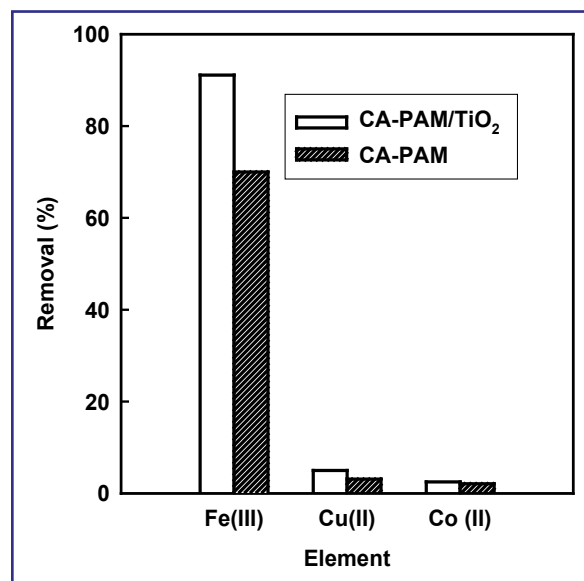

Fig. (10): Removal % of Fe (III), Co (II) and Cu (II) by CA/PAM and CA/PAM/TiO$_2$ nanocomposite films in mixture solution of the three metal ions. The Initial concentration 30 ppm for each metal, pH; 3, TiO$_2$ content; 0.3 wt%, time of adsorption; 2h at 25°C.

It is observed that both CA-PAM and CA-PAM/TiO$_2$ nanocomposite films exhibit low removal % of Cu (II) and Co (II) with relatively high removal % of Fe (III) and Table 3 represents the adsorption capacity of metal ions in competitive adsorption.

Table (3) : *Adsorption capacity of Fe (III), Co (II), and Cu (II) in competitive adsorption.*

Element	CA-PAM/TiO$_2$	CA-PAM
Fe(III)	5.5	3.8
Cu (II)	0.8	1.1
Co (II)	0.4	0.4

Adsorption selectivity parameters; distribution coefficient (K_d) and selectivity coefficient (k) were calculated and results are summarized in tables 4 and 5.

Table (4) : *Distribution coefficient.*

K_d(mL/g)	Fe (III)	Cu (II)	Co (II)
CA-PAM	0.4	0.03	0.01
CA-PAM/TiO$_2$	2.2	0.04	0.01

Table (5) : *Selectivity coefficient.*

K	Fe(III)/Cu(II)	Fe(III)/Co(II)
CA-PAM	13.3	40
CA-PAM/TiO$_2$	55	220

It was observed that the adsorption capacity and the distribution coefficient of Fe (III) is greater than that of Cu (II) and Co (II) for CA-PAM and CA-PAM/TiO$_2$ nanocomposites due to lower amount adsorbed of Cu (II) and Co (II) at low pH with high adsorption of Fe (III). It is also observed that selectivity coefficient for CA-PAM/TiO$_2$ nanocomposite film is greater than that for CA-PAM due to improve the surface area and abundant functional groups in the nanocomposites which able to bind Fe (III) and create more selective recognition sites make CA-PAM/TiO$_2$ more efficient in selective adsorption of Fe (III).

CONCLUSION

CA-PAM/TiO$_2$ nanocomposite films were prepared with different contents of TiO$_2$ nanoparticles 0-0.5 (wt%) using gamma radiation as initiator. Crystallite size obtained from XRD analysis confirmed incorporation of nanoparticle within polymer matrix. SEM reveals that, TiO$_2$ creates a porous structure in CA-PAM/TiO$_2$ nanocomposite films. Removal % of Fe (III) was studied as a function of TiO$_2$ content, pH, time of adsorption, initial concentration, temperature and number of adsorption cycles. Incorporation of TiO$_2$ in CA-PAM 50/50 (wt%) improves Fe (III) removal percent from 68 to 91 as compared with CA-PAM film. Adsorption reached equilibrium in short time which is important factor in adsorption behavior. Thermodynamic study showed that the adsorption is chemisorption and endothermic in nature. Reusability studies indicated that CA-PAM/TiO$_2$ films maintain 90% of their efficiency after four regeneration cycles while CA-PAM maintains only 50%. Selective adsorption studies of Fe(III) in presence of other interfering metal ions clarified that CA-PAM/TiO$_2$ nanocomposite film more efficient in selective adsorption of Fe (III) and exhibited higher selectivity coefficient than CA-PAM films.

REFERENCES

- **Abou Taleb, M.F.; Abd El-Mohdy, H.L. and Abd El-Rehim, H.A. (2009):** Radiation preparation of PVA/CMC copolymers and their application in removal of dyes. *Hazard. Mater. J.*, 168: 68

- **Atta, A.; Al-lohedan, H.; Tawfffk, A. and Abdel-Khalek, A. (2016):** Preparation and characterization of amphilic Titanium dioxide nanogel composite with high performance in waste water treatment. *DIG NANOMETER BIOS J.*, 11: 91

- **Benavides, S.; Villalobos-Carvajal, R. and Reyes, J. (2012):** Physical, mechanical and antibacterial properties of alginate film: Effect of the crosslinking degree and oregano essential oil concentration. *J. Food. Eng,.* 110: 232

- **Borai, E.; Breky, M.; Sayed, M. and Abo-Aly, M. (2015):** Synthesis, characterization and application of titanium oxide nanocomposites for removal of radioactive cesium, cobalt and europium ions**.** *J. Colloid Interface Sci.*, 450: 17

- **Bouhamed, F.; Elouear, Z.; Bouzid, J. and Ouddane, B. (2014):** Multi-component adsorption of copper, nickel and zinc from aqueous solutions onto activated carbon prepared from date stones. International conference on integrated management of the environment- ICIME

- **Cerqueira, M.; Souza, B.; Teixeira, J. and Vicente, A. (2012):** Effect of glycerol and corn oil on physicochemical properties of polysaccharide films - A comparative study" *Food Hydrocolloids J.*, 27: 175

- **Dey, K.; Ganguli, S.; Ghoshal, S.; Khan, M. and Khan, R. (2014):** Study of the Effect of Gamma Irradiation on the Mechanical Properties of Polyvinyl Alcohol Based Gelatin Blend Film. *OAL.J.*, 1: e639

- **Eisa, W.; Abdel-Moneam, Y.; Shaaban, Y.; Abdel-Fattah, A. and Abou Zeid, A. (2011):** Gamma-irradiation assisted seeded growth of Ag nanoparticles within PVA Matrix. *Mater. Chem. Phys.*, 128: 109

- **El Miri, N.; Abdelouahdi, K.; Zahouily, M.; Fihri, A.; Barakat, A.; Solhy, A. and El Achaby, M. (2015):** Bio-nanocomposite films based on cellulose nanocrystals filled polyvinyl alcohol/chitosan polymer blend. *J. APPL. POLYM. SCI.*, 42004: 1

- **El Sayed, A.; El-Gamal, S.; Morsi, W. and Mohammed, G. (2015):** Effect of PVA and copper oxide nanoparticles on the structural, optical, and electrical properties of carboxymethyl cellulose films. *J Mater Sci*. 50:4717

- **Foox, M.; Ben-Tzur, M.; Koifman, N.; and Zilberman, M. (2016):** Effect of gamma radiation on novel gelatin alginate–based bioadhesives *Int. J. Polym. Mater. Polym. Biomater.*, 65: 611

- **Golkhah, S.; Mousavi, H. Z.; Shirkhanloo, H.; and Khaligh, A. (2017):** Removal of Pb (II) and Cu(II) Ions from Aqueous Solutions by Cadmium Sulfide Nanoparticles. *Int. J. Nanosci. Nanotechnol.*, 13:105

- **Habiba, U.; Afifi, A.M.; Salleh, A. and Ang, B.C. (2016):** Chitosan/(polyvinyl alcohol)/zeolite electrospun composite nanofibrous membrane for adsorption of Cr^{6+}, Fe^{3+} and Ni^{2+}. *J. Hazard. Mater.*,06:028

- **Karkeh-abadi, F.; Saber-Samandari, S. and Saber-Samandari, S. (2016):** The impact of functionalized CNT in the network of sodium alginate-based nanocomposite beads on the removal of Co(II) ions from aqueous solutions. *J. Hazard. Mater.*, 312:224

- **Mittal, A.; Ahmad, R. and Hasan, I. (2015):** Poly (methyl methacrylate)-grafted alginate/Fe_3O_4 nanocomposite: synthesis and its application for the removal of heavy metal ions. *Desalination and Water Treatment J.,* 1:14

- **Moniera, M.; Ibrahim, A.; Metwally, M. and Badawyca, D. (2015):** Surface ion-imprinted amino-functionalized cellulosic cotton fibers for selective extraction of Cu(II) ions. *Int. J. Bio. Macromol.*, 81: 736

- **Norranattrakul, P.; Siralertmukul, K. and Nuisin, R. (2013):** Fabrication of chitosan/titanium dioxide composites film for the photocatalytic degradation of dye. *J.Metals, Materials and Minerals.*, 23: 9

- **Oleyaei, S.; Zahedi, Y.; Ghanbarzadehd, B. and Moayedi, A. (2016):** Modification of physicochemical and thermal properties of starch films by incorporation of TiO_2 nanoparticles.*Int. J. Bio. Macromol.*, 89:256

- **Pal, A.; Das, D.; Sarkar, A.; Ghorai, S.; Das, R. and Pal, S. (2015):** Synthesis of glycogen and poly (acrylic acid)-based graft copolymers via ATRP and its application for selective removal of Pb^{2+} ions from aqueous solution. *Eur. Polym. J.*, 66: 33

- **Paranhos, C.M.; Soares, B.G.; Machado, J.; Windm□ller, D. and Pessan, L.A. (2007):** Microstructure and free volume evaluation of poly(vinyl alcohol) nanocomposite hydrogels. *Eur. Polym. J.,* 43: 4882.

- **Peters, R.; Bemmel, G.; Herrera-Rivera, Z.; Helsper, J.; Marvin, H.; Weigel, S.; Tromp, P.; Oomen, A.; Rietveld, A. and Bouwmeester, H. (2014):** Characterisation of titanium dioxide nanoparticles in food products: Analytical methods to define nanoparticles. *J.Agric. Food. Chem.*, 1:34

- **Poursani, A.; Nilchi, A.; Hassani, A.; Shariat, S. and Nouri1, J. (2016):** The Synthesis of Nano TiO_2 and Its Use for Removal of Lead Ions from Aqueous Solution. *J. Water Resource and Protection.*, 8: 438-

- **Quintelas, C.; Rocha, Z.; Silva, B.; Fonseca, B.; Figueiredo, H. and Tavares, T. (2009):** Removal of Cd(II), Cr(VI), Fe(III) and Ni(II) from aqueous solutions by an E. coli biofilm supported on kaolin. *Chem. Eng. J.*, 149:319

- **Rhim, J. and Wang, L. (2013):** Mechanical and water barrier properties of agar/κ-carrageenan/konjac glucomannan ternary blend biohydrogel films. *Carbohydr. Polym.,* 96: 71

- **Selçuk, N.C.; Kubilay, S.; Savran, A. and Kul, A.R. (2017):** Kinetics and Thermodynamic Studies of Adsorption of Methylene Blue from Aqueous Solutions onto Paliurus spina-christi Mill. Frutis and Seeds. *J.App. Chem.,* 10: 53

- **Teke, M.; Mercimek, B.; Ozler, M.A. and Ayar, A. (2004):** Selective extraction of Iron (III) from aqueous solution in presence of Cobalt (II), Copper (II), Nickel (II) using Bis(Δ2-2-Imidazolinyl)-5,5'-dioxime. *Anal. Sci.,* 20: 853

- **Thakur, S. (2017):** Synthesis, characterization and adsorption studies of an acrylic acid-grafted sodium alginate-based TiO_2 hydrogel nanocomposite**.** *Adsorpt. Sci. Technol*., 0(0): 1

- **Xie, F.; Liua, G.; Wu, F.; Guo, G. and Li, G. (2012):** Selective adsorption and separation of trace dissolved Fe (III) from natural water samples by double template imprinted sorbent with chelating diamines**.** *Chem. Eng. J.,* 183:372.

- **Yin, J. and Deng, B. (2015):** Polymer-matrix nanocomposite membranes for water treatment. *J. Membr. Sci.,* 479: 256.